High Input Voltage High Frequency Class E Rectifiers for Resonant Inductive Links

Samer Aldhaher, Patrick C. K. Luk, *Senior Member, IEEE*, Khalil El Khamlichi Drissi,
James F. Whidborne, *Senior Member, IEEE*

Abstract—The operation of traditional rectifiers such as half-wave and bridge rectifiers in wireless power transfer applications may be inefficient and can reduce the amount of power that is delivered to a load. An alternative is to use Class E resonant rectifiers which are known to operate efficiently at high resonant frequencies and at large input voltages. Class E rectifiers have a near sinusoidal input current which leads to an improved overall system performance and increased efficiency, especially that of the transmitting coil driver. This paper is the first to investigate the use of Class E resonant rectifiers in wireless power transfer systems based on resonant inductive coupling. A piecewise linear state-space representation is used to model the Class E rectifier including the rectifying diode's forward voltage drop, its ON resistance and the equivalent series resistance of the resonant inductor. Power quality parameters, such as power factor and total harmonic distortion, are calculated for different loading conditions. Extensive experimental results based on a $10\,\mathrm{W}$ prototype are presented to confirm the performed analysis and the efficient operation of the rectifier. An impressive operating efficiency of $94.43\,\%$ has been achieved at a resonant frequency of $800\,\mathrm{kHz}$.

Index Terms—Inductive power transmission, AC-DC power converters, high frequency rectifiers.

I. Introduction

Whilst most of recent published work in inductive power transfer (IPT) technology focuses on the design and optimization issues of the resonant inductive coils [1]–[8] and the transmitting coil driver [9]–[13], there has been little research in high frequency, high efficiency rectifiers for IPT applications and their impact on the overall performance of an IPT system. In previous papers, the load connected to the secondary coil of the inductive link has either been an AC load in the form of a resistor [1], [2], [8]–[14], or a DC load connected through an AC/DC rectifier. Since DC loads are more common than AC loads, more research into rectifiers that are suitable for IPT systems is required.

The majority of AC/DC rectifiers that have been used in recent publications about IPT systems are either traditional half-wave rectifiers [15] or bridge rectifiers [3], [7], [16], [17]. The main losses that occur in the rectifiers are due to the forward voltage drop of the rectifying elements and their switching losses. Synchronous rectifiers based on a bridge configuration can improve the overall efficiency in IPT systems. However timing and control of the four switches may be difficult especially at high resonant frequencies [18]. In addition, traditional half-wave rectifiers and bridge rectifiers have a non-sinusoidal input current and can cause a non-sinusoidal current to flow out of the secondary resonant circuit of the inductive link. This affects the performance and efficiency of the primary coil driver since most primary coil drivers operate at resonance and generate a sinusoidal driving current.

Class E rectifiers are resonant switching circuits that can operate efficiently at frequencies exceeding $500\,\mathrm{kHz}$. Efficient operation is achieved due to the zero-voltage switching (ZVS), low voltage-slope (dv/dt) switching, zero-current switching (ZCS) and low current-slope (di/dt) switching of the rectifying element. The principle of operation of Class E rectifiers and the different configurations that have been researched are summarised in [19], [20] and the references therein. Class E rectifiers have a near sinusoidal input current with low harmonic distortion which makes them compatible with resonant inverters, such as Class D and Class E, that are used as primary coil drivers in IPT systems. Class E rectifiers have been used to form resonant DC-DC converters [21]–[26] and in power harvesting and power recovery applications [27]. Nonetheless, there appears no report in literature on the use of Class E rectifiers for IPT systems.

This paper is the first to propose and implement a Class E rectifier for IPT. Here, a Class E half-wave ZVS, low dv/dt resonant switching rectifier is developed for IPT systems with a parallel resonant secondary coil to improve their performance and increase their overall efficiency. Based on the well established Class E rectifier configuration in [28], this paper extends the work by introducing a novel analysis based on state-space modelling to provide a more accurate mathematical representation of the rectifier. The state-space model takes into consideration the diode forward voltage drop, its ON resistance and the equivalent series resistance (ESR) of the resonant inductor, all of which have been omitted in the analysis of Class E rectifiers in previous work.

This paper is organised as follows. Section II introduces the Class E rectifier and presents a piecewise linear state-space model, parameters such as duty cycle and output voltage are numerically evaluated. Section III discusses the performance of the Class E rectifier by evaluating several parameters which haven't been evaluated before for Class E rectifiers such as the power factor, the normalised input root mean square (RMS) current and its total harmonic distortion (THD). Section IV presents extensive experimental results about the operation and the performance of a Class E rectifier used in an IPT system. Section V gives the conclusion and suggests future work.
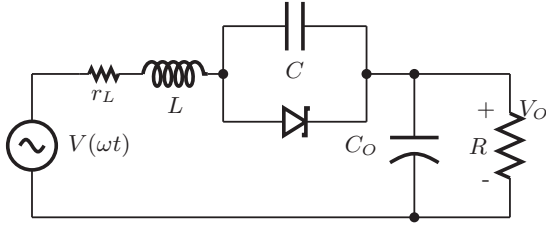
Fig. 1. Circuit diagram of the Class E ZVS low dv_d/dt rectifier with a rectifying diode.

(a)

(b)

Fig. 2. Equivalent circuits (a) ON period (b) OFF period.

II. MODELLING AND ANALYSIS

A. Class E low ZVS, low dv/dt rectifier

The circuit of the Class E rectifier is shown in Fig. 1 with a Schottky diode as the rectifying element. Capacitor C, referred to as the resonant capacitor, is connected in parallel with the diode. Inductor L, referred to as the resonant inductor, is connected in series with the resonant capacitor and the diode, r_L represents the equivalent series resistance (ESR) of the resonant inductor. The ESR of the resonant capacitor is assumed to be negligible. The load resistance R represents the output load and an output capacitor C_O is connected across the load. Capacitor C_O should be large enough such that the output voltage V_O is DC and ripple free. The input voltage V is sinusoidal and can represent the output voltage of the receiving coil of an IPT system. The resonant frequency of L and C is equal to the frequency of the input voltage given as

$$\omega = \frac{1}{\sqrt{LC}}. \tag{1}$$

The characteristic impedance of the resonant circuit is

$$Z = \omega L = \frac{1}{\omega C} = \sqrt{\frac{L}{C}} \tag{2}$$

and the normalised load is

$$R_{\text{norm}} = \frac{R}{Z}. \tag{3}$$

B. State-Space Representation

The equivalent circuits are shown in Figs. 2a and 2b for the ON and OFF periods respectively. The piecewise linear model of a diode is used which consists of a voltage source V_f, representing the forward voltage drop, and resistance r_{ON}, representing the diode's ON resistance. The equivalent circuits are a piecewise linear multiple input multiple output time invariant system which can be represented by the following state-space representation for each ON and OFF intervals

$$\dot{\mathbf{x}}(\omega t) = A\mathbf{x}(\omega t) + B\mathbf{u}(\omega t) \tag{4}$$
$$\mathbf{y}(\omega t) = C\mathbf{x}(\omega t) + D\mathbf{u}(\omega t) \tag{5}$$

where $\mathbf{x}(\omega t) = [x_1(\omega t), x_2(\omega t), x_3(\omega t)]^T$ is the state vector. The state variables x_1, x_2, x_3 represent the current through inductor L, the voltage across capacitor C and the voltage across capacitor C_o for both ON and OFF intervals respectively. The input vector $\mathbf{u}(\omega t) = [u_1(\omega t), u_2(\omega t)]^T$ where u_1 and u_2
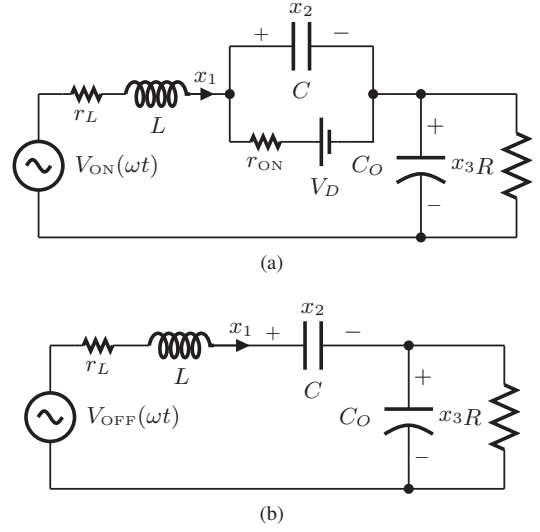
represent the input sinusoidal voltage and the forward voltage drop of the diode respectively. The ON interval's domain is defined as $0 \le \omega t \le 2\pi D$ and the OFF interval's domain is defined as $0 \le \omega t \le 2\pi(1 - D)$ where D is the ON duty cycle of the diode. Using KVL and KCL, the matrices A, B, C and D and the input vectors, denoted by the subscripts ON and OFF for both intervals are given as

$$A_{\text{ON}} = \begin{bmatrix} \dfrac{-r_L}{\omega L} & \dfrac{-1}{\omega C} & \dfrac{-1}{\omega L} \\ \dfrac{1}{\omega C} & 0 & 0 \\ \dfrac{1}{\omega C_O} & 0 & \dfrac{-1}{\omega R C_O} \end{bmatrix} \tag{6}$$

$$A_{\text{OFF}} = \begin{bmatrix} \dfrac{-r_L}{\omega L} & \dfrac{-1}{\omega C} & \dfrac{-1}{\omega L} \\ \dfrac{1}{\omega C} & \dfrac{-1}{\omega r_{\text{ON}} C} & 0 \\ \dfrac{1}{\omega C_O} & 0 & \dfrac{-1}{\omega R C_O} \end{bmatrix} \tag{7}$$

$$B_{\text{ON}} = \begin{bmatrix} B_{1\text{ON}} & B_{2\text{ON}} \end{bmatrix} = \begin{bmatrix} \dfrac{1}{\omega L} & 0 \\ 0 & \dfrac{1}{\omega r_{\text{ON}} C} \\ 0 & 0 \end{bmatrix} \tag{8}$$

$$B_{\text{OFF}} = \begin{bmatrix} B_{1\text{OFF}} & B_{2\text{OFF}} \end{bmatrix} = \begin{bmatrix} \dfrac{1}{\omega L} & 0 \\ 0 & 0 \\ 0 & 0 \end{bmatrix} \tag{9}$$

$$C_{\text{ON}} = C_{\text{OFF}} = \begin{bmatrix} 1 & 0 & 0 \\ 0 & 1 & 0 \\ 0 & 0 & 1 \end{bmatrix} \tag{10}$$

$$D_{\mathrm{ON}} = D_{\mathrm{OFF}} = \begin{bmatrix} 0 & 0 \\ 0 & 0 \\ 0 & 0 \end{bmatrix} \quad (11)$$

$$\mathbf{u}_{\mathrm{ON}}(\omega t) = \begin{bmatrix} u_{1\mathrm{ON}}(\omega t) \\ u_{2\mathrm{ON}}(\omega t) \end{bmatrix} = \begin{bmatrix} v_m \sin(\omega t + \phi_{\mathrm{ON}}) \\ V_f \end{bmatrix} \quad (12)$$

$$\mathbf{u}_{\mathrm{OFF}}(\omega t) = \begin{bmatrix} u_{1\mathrm{OFF}}(\omega t) \\ u_{2\mathrm{OFF}}(\omega t) \end{bmatrix} = \begin{bmatrix} v_m \sin(\omega t + \phi_{\mathrm{OFF}}) \\ 0 \end{bmatrix} \quad (13)$$

where v_m is the magnitude of the input voltage and

$$\phi_{\mathrm{ON}} = \phi_o + 2\pi(1 - D) \quad (14)$$
$$\phi_{\mathrm{OFF}} = \phi_o. \quad (15)$$

The solution to Eq. 4 for both ON and OFF states is

$$\mathbf{x}(\omega t) = \mathbf{x_n}(\omega t) + \mathbf{x_f}(\omega t). \quad (16)$$

Function $\mathbf{x_n}$ is the natural response, or the zero-input response, and is equal to

$$\mathbf{x_n}(\omega t) = e^{A\omega t}\mathbf{x}(0) \quad (17)$$

where $\mathbf{x}(0)$ is the initial condition of the states, e is the matrix exponential function. Function $\mathbf{x_f}$ is the forced response, or the zero-state response, and is equal to

$$\mathbf{x_f}(\omega t) = \int_0^\tau e^{A(\omega t - \tau)} B\mathbf{u}(\tau)d\tau$$
$$= \int_0^{\omega t} e^{A(\omega t - \tau)} \begin{bmatrix} B_1 & B_2 \end{bmatrix} \begin{bmatrix} u_1(\tau) \\ u_2(\tau) \end{bmatrix} d\tau$$
$$= \int_0^{\omega t} e^{A(\omega t - \tau)} \big(B_1 u_1(\tau) + B_2 u_2(\tau)\big)d\tau$$
$$= (A^2 + \mathbf{I})^{-1}\Big(e^{A\omega t}\big(\mathbf{I}\cos(\phi) + A\sin(\phi)\big)$$
$$- \mathbf{I}\cos(\omega t + \phi) - A\sin(\omega t + \phi)\Big)B_1 + A^{-1}\big(e^{A\omega t} - \mathbf{I}\big)B_2 \quad (18)$$

where τ is a dummy variable and $\mathbf{I}$ is a 3×3 identity matrix.

The initial conditions of the states can be determined by applying the continuity conditions of the current through L and the voltages across C and C_O when circuit transitions from the ON state to the OFF state, hence the following equations are obtained

$$\mathbf{x}_{\mathrm{ON}}(0) = \mathbf{x}_{\mathrm{OFF}}(2\pi(1 - D)) \quad (19)$$
$$\mathbf{x}_{\mathrm{OFF}}(0) = \mathbf{x}_{\mathrm{ON}}(2\pi D). \quad (20)$$

By evaluating Eqs. 19 and 20, the initial conditions can be solved for as follows

$$\begin{bmatrix} \mathbf{x}_{\mathrm{ON}}(0) \\ \mathbf{x}_{\mathrm{OFF}}(0) \end{bmatrix} = \begin{bmatrix} -e^{A_{\mathrm{ON}}2\pi D} & \mathbf{I} \\ \mathbf{I} & -e^{A_{\mathrm{OFF}}2\pi(1-D)} \end{bmatrix}^{-1} \cdot$$
$$\begin{bmatrix} \mathbf{x_{fON}}(2\pi D) \\ \mathbf{x_{fOFF}}(2\pi(1 - D)) \end{bmatrix}. \quad (21)$$

The values of D and ϕ can be numerically solved for by finding the instants at which the voltage across the diode is equal to zero in both ON and OFF intervals, i.e

$$x_{2\mathrm{ON}}(0) - V_f = 0 \quad (22)$$
$$x_{2\mathrm{OFF}}(0) - V_f = 0. \quad (23)$$

Fig. 3 shows the solved values of D, ϕ and the normalised output DC voltage $V_{O\mathrm{norm}}$ with respect to the peak input voltage for an ideal Class E inverter with $V_f = 0$, $r_{\mathrm{ON}} = 0$ and $r_L = 0$. The ON duty cycle of diode is high for lower normalised loads and declines as the normalised load increases. The duty cycle at a normalised load of unity is 0.403, it increases by approximately 50 % as the normalised load is reduced to 0.1 and decreases by more than 50 % as the normalised load increases to 10. The normalised output voltage increases as the load increases at lower duty cycles, and decreases as the load is reduced at lower duty cycles. The output voltage is approximately a linear function of the load.

It is noted that the results in Fig. 3 match the results obtained using the analytical approach in [28]. Therefore, the validity and accuracy of the state-space modelling approach are confirmed.

III. INPUT CURRENT LINEARITY AND HARMONIC CONTENT

It is necessary to investigate the signal quality of the input current of the Class E rectifier in order to determine its performance and suitability to be used in a resonant IPT system. The main parameters of interest are the normalised RMS value of the input current with respect to the output current, the power factor (PF) and the total harmonic distortion of the input current. These parameters will be derived for the ideal Class E rectifier ($V_f = 0$, $r_{\mathrm{ON}} = 0$ and $r_L = 0$) in order to provide a reference case that will show how they will be affected by the duty cycle and load.

A. Input RMS current

The RMS values of the input current, the voltage across capacitor C, the diode's voltage and the voltage across the output capacitor C_O can be calculated by evaluating the RMS value of the state vector $\mathbf{x}(\omega t)$ in Eq. 16 as shown below

$$\begin{bmatrix} I_{L\mathrm{RMS}} & V_{C\mathrm{RMS}} & V_{O\mathrm{RMS}} \end{bmatrix}^T = \mathbf{x}_{\mathrm{RMS}} =$$
$$\sqrt{\frac{1}{2\pi}\left(\int_0^{2\pi D} \mathbf{x}_{\mathrm{ON}}^{\circ 2}(\omega t)d\omega t + \int_0^{2\pi(1-D)} \mathbf{x}_{\mathrm{OFF}}^{\circ 2}(\omega t)d\omega t\right)}. \quad (24)$$

(a) Duty cycle against normalised load

(b) Phase angle against normalised load

(c) Phase angle against duty cycle

(d) Normalised output voltage against normalised load
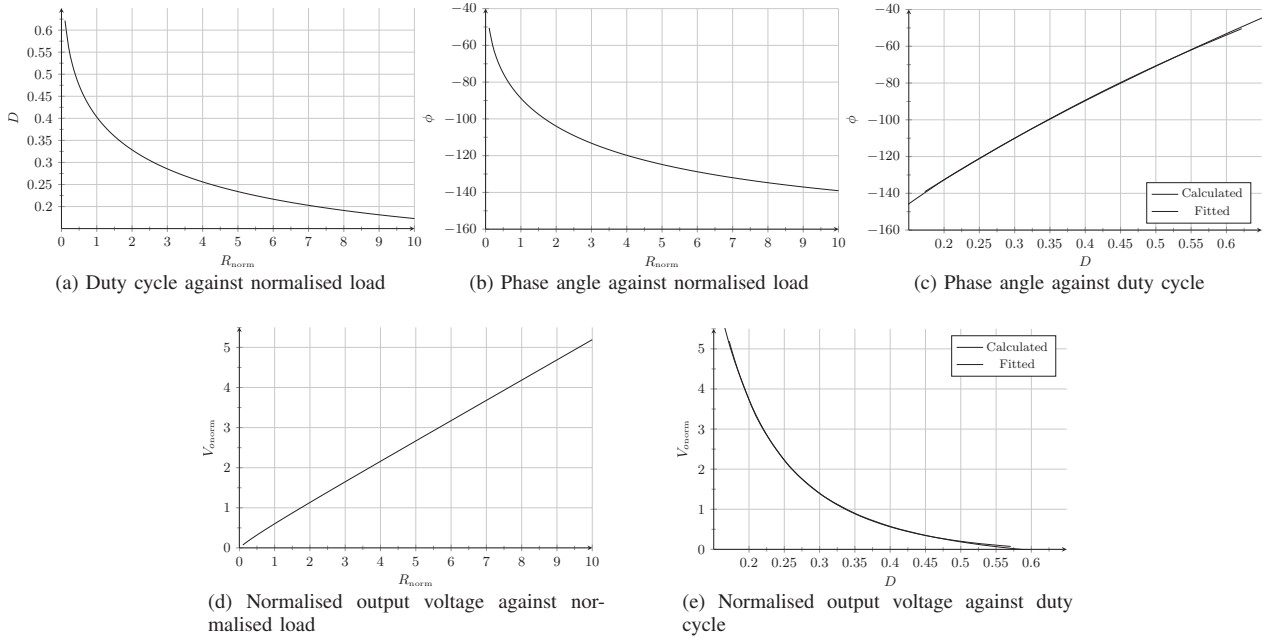
(e) Normalised output voltage against duty cycle

Fig. 3. Numerically calculated values.

Figs. 4a and 4d show the normalised input RMS current as a function of the duty cycle and the normalised load respectively for the ideal Class E rectifier. The input RMS current is lower for low normalised loads at higher duty cycles. This is because the rectifier behaves more as an inductive load since the diode is ON for most of the switching period. The input RMS current increases as the normalised load increases at lower duty cycles since the rectifier operates at resonance and therefore has a reduced input impedance.

B. Power factor

The power factor can be used as an indication of how reactive the reflected impedance of the rectifier is for different loading conditions as seen from the receiving and transmitting coils of a resonant IPT system. As the Class E rectifier generally presents an inductive load to the source, it can detune the IPT system from operating at resonance. Consequently, finding the power factor can aid in determining the type of compensation required to retune the IPT system to operate at resonance and its optimal location to be in the IPT system. The power factor is defined as the ratio of the real power to the apparent power at the input of a system. For the Class E rectifier, the power factor can be expressed as

$$\text{PF} = \frac{P_{\text{IN}}}{v_m I_{\text{RMS}}} \quad (25)$$

where P_{IN} is the input real power and is equal to the sum of the power delivered to the load, the power lost in the diode's forward voltage and its ON resistance and the power lost due to the ESR of inductor L. Hence, the input real power can be expressed as

$$P_{\text{IN}} = \frac{V_{O\text{RMS}}}{R}\left(V_{O\text{RMS}} + V_f + \frac{V_{O\text{RMS}}}{R}r_{\text{ON}}\right) + I_{L\text{RMS}}^2 r_L. \quad (26)$$

Note that the RMS value of the output voltage is equal to its mean or DC value.

Figs. 4b and 4e show the variation of the power factor with duty cycle and normalised load respectively for the ideal Class E rectifier. The power factor approaches unity for higher normalised loads at low duty cycles since the diode is switched OFF for most of the switching period. The rectifier operates mostly at resonance and therefore has a higher power factor. The power factor decrease to zero for lower normalised loads at higher duty cycles since the diode is switched ON for most of the switching period. The rectifier behaves more as an inductive circuit and therefore the power factor is reduced. Depending on the load, a passive compensation circuit can be included at the receiver of the IPT system for a fixed load or at the transmitter for a variable load.

C. Total harmonic distortion

As mentioned previously, a high harmonic content in the input current of the rectifier can disrupt the resonant operation of the transmitting coil driver in a resonant inductive link. The total harmonic distortion (THD) of the Class E rectifier is given by

$$\text{THD} = \frac{\sqrt{\sum_{n=2}^{\infty} i_{Ln}^2}}{i_{L1}} \quad (27)$$

where i_{L1} is the fundamental current component of the input current at the resonant frequency and i_{Ln} represents the input current harmonics. Using the Fourier trigonometric series formula, i_{Ln} can be derived by evaluating the harmonic content

of the state vector $\mathbf{x}(\omega t)$ in Eq. 16 as shown below

$$\begin{bmatrix} i_{Ln} & v_{cn} & v_{C_o n} \end{bmatrix}^T = \mathbf{x}_n = \left(\mathbf{a}_n^{\circ 2} + \mathbf{b}_n^{\circ 2}\right)^{\circ \frac{1}{2}}. \quad (28)$$

The coefficients matrices $\mathbf{a}_n$ and $\mathbf{b}_n$ contain the Fourier coefficients and are equal to

$$\mathbf{a}_n = \frac{1}{\pi}\left(\int_0^{2\pi D} \mathbf{x}_{\text{ON}}(\omega t)\cos\left(n\omega t + \phi + 2\pi(1-D)\right)d\omega t + \int_0^{2\pi(1-D)} \mathbf{x}_{\text{OFF}}(\omega t)\cos\left(n\omega t + \phi\right)d\omega t\right) \quad (29)$$

$$\mathbf{b}_n = \frac{1}{\pi}\left(\int_0^{2\pi D} \mathbf{x}_{\text{ON}}(\omega t)\sin\left(n\omega t + \phi + 2\pi(1-D)\right)d\omega t + \int_0^{2\pi(1-D)} \mathbf{x}_{\text{OFF}}(\omega t)\sin\left(n\omega t + \phi\right)d\omega t\right) \quad (30)$$

Figs. 4c and 4f show the variation the THD of the input current with duty cycle and normalised load for the ideal Class E rectifier. The THD has a peak value of $10.34\,\%$ at a duty cycle of 0.392 and normalised load of 1.10. The THD is reduces when the duty cycle approaches zero or unity since the diode is either ON or OFF for most of the switching period and the effect of the rectifier transitioning from either the ON and OFF states is reduced.

IV. Experimental Setup and Results

A Class E rectifier has been built to deliver up to $10\,\text{W}$ for a previously designed IPT system presented in [9]. The IPT system, shown in Fig. 5, consists of a Class E resonant inverter as the transmitting coil's current driver, an inductive link formed by a transmitting coil and a receiving coil that are aligned with each other and separated by a distance of $5\,\text{cm}$. A capacitor is connected across the receiving coil to form a parallel LC tank to boost the voltage induced at the receiving coil. The parallel LC configuration is generally used in wireless power systems where energy is to be transferred across a large gap. High voltage levels that can reach up to several hundreds of volts can be generated at low current levels, therefore ohmic losses are minimised. The values of the LC tank were chosen to set its resonate frequency at $800\,\text{kHz}$ to maximise the efficiency of the inductive link. A photograph of the complete system is shown in Fig. 6.

The rectifier was designed to operate at a duty cycle of 0.5 for maximum power capability [28] and its resonant frequency is designed to match the operating frequency of the IPT system which is at $800\,\text{kHz}$. The values of the load resistance R is $77.5\,\Omega$, the resonant inductor L is $39.5\,\mu\text{H}$, the resonant capacitor C is $1\,\text{nF}$ and the output capacitor C_O is $1\,\mu\text{F}$. The Schottky diode used is SB3100 (100V/3A), its forward voltage drop is $0.3\,\text{V}$ and its ON resistance is $0.45\,\Omega$. The resonant inductor consists of 64 turns wound on a T68-7B core from Mircometals and its ESR is $0.5\,\Omega$. The input voltage to the IPT system is varied to control the induced voltage that is to be rectified at the receiving coil.

The principle of operation of this setup can be described as follows. Since the transmitting coil of the inductive link is driven by the current output of the Class E inverter, the receiving coil of the inductive link will behave as a constant current source. The voltage across the parallel capacitor, which its value was chosen to resonate with the receiving coil, increases accordingly with time which in turn drives the Class E rectifier. The output current of the rectifier increases and the voltage across the load increases. The input power to the rectifier will increase in proportion with the output voltage across the resonant capacitor, however the power to load increases with square of the load's voltage. The input power to the rectifier will cease to increase once it is equal to the load's power and the input voltage to the rectifier and the load's voltage will be held. A large portion of the input voltage will be dropped across the resonant inductor L and its values controls the rectifier's input current harmonics.

Figs. 7a and 7b show the measured and calculated output voltage and input RMS current of the rectifier respectively as the input voltage to the rectifier varies from $20\,\text{Vpp}$ to $200\,\text{Vpp}$. The calculated voltage gain of the rectifier is approximately $26\,\%$ over the entire input voltage range. The voltage gain is lower than that of other rectifiers such as the traditional bridge rectifier. For high frequency IPT systems the expected loads are low power DC devices that operate between $5\,\text{V-}12\,\text{V}$. Therefore the low voltage gain of the presented Class E rectifier can allow for DC loads to be powered directly from the rectifier without the need of any DC/DC conversion. Fig. 7c compares the measured and calculated power factors, and shows that they deviate slightly over the entire input voltage range. In Fig. 7d, the measured and calculated input and output powers are both shown to be compared favourably. Fig. 7e shows slight deviation between the measured and calculated efficiencies. It is shown that the Class E rectifier has a maximum efficiency of $94.43\,\%$ at an input voltage of $100\,\text{Vpp}$ and is above $90\,\%$ over most of the input voltage range. The calculated variation of the duty cycle is shown in Fig. 7f.

Fig. 8 shows the measured and simulated voltage and current waveforms throughout the rectifier for an input voltage of $200\,\text{Vpp}$. Fig. 8a shows the measured input voltage that is induced at the receiving coil. It can be seen that the input voltage can be considered to be sinusoidal when compared to the reference sinusoidal plot. The measured and simulated input currents are shown in Fig. 8b, the input current is a near sinusoidal and contains a DC offset current. The obtained and simulated diode voltage and current waveforms are shown in Figs. 8c and 8d respectively. The ringing observed in diode's current is due to the lead inductances of the diode and the current probe. Fig. 8e shows the magnitude of the first four harmonic contents of the measured and simulated input currents. The THD of the measured input current is $8.84\,\%$ compared to a calculated value of $8.89\,\%$. The overall excellent agreements between all the measured and calculated results confirm the validity of the analysis and the modelling approach.

V. Conclusions and Future Work

This paper presents a high input voltage high efficiency ZVS, low dv/dt Class E rectifier to be used in resonant

(a) Normalised RMS input current against duty cycle

(b) Power factor against duty cycle

(c) THD against duty cycle

(d) Normalised RMS input current against normalised load

(e) Power factor against normalised load
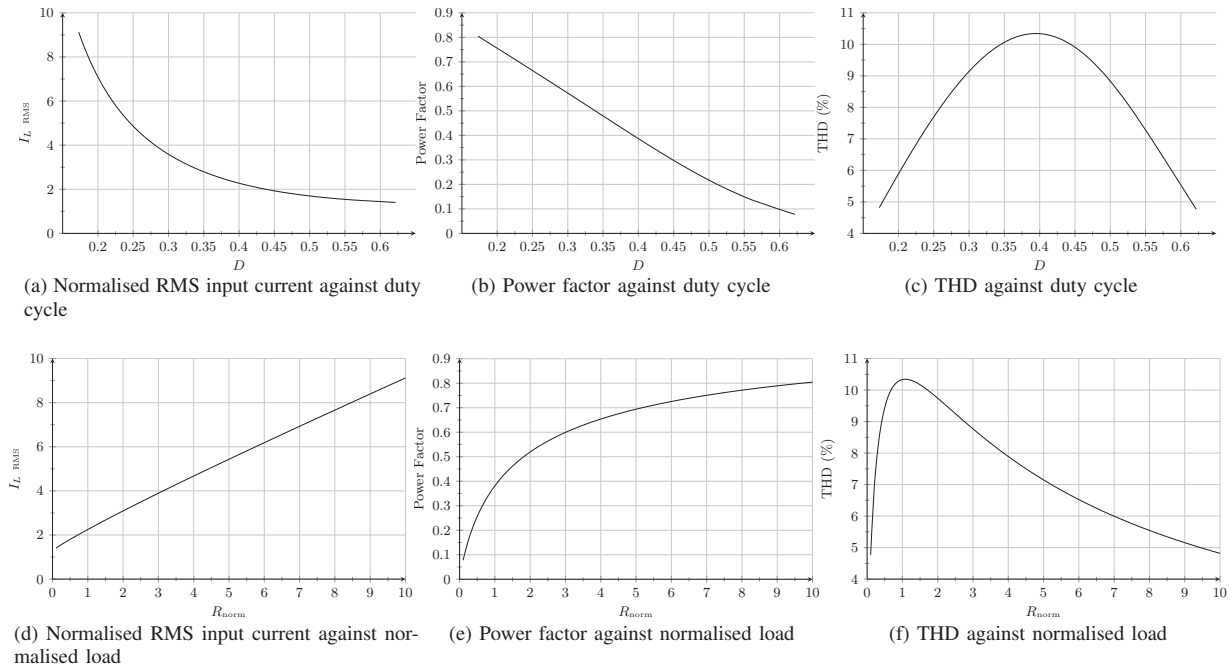
(f) THD against normalised load

Fig. 4. Power quality parameters for the ideal Class E rectifier at different duty cycle and normalised load combinations.

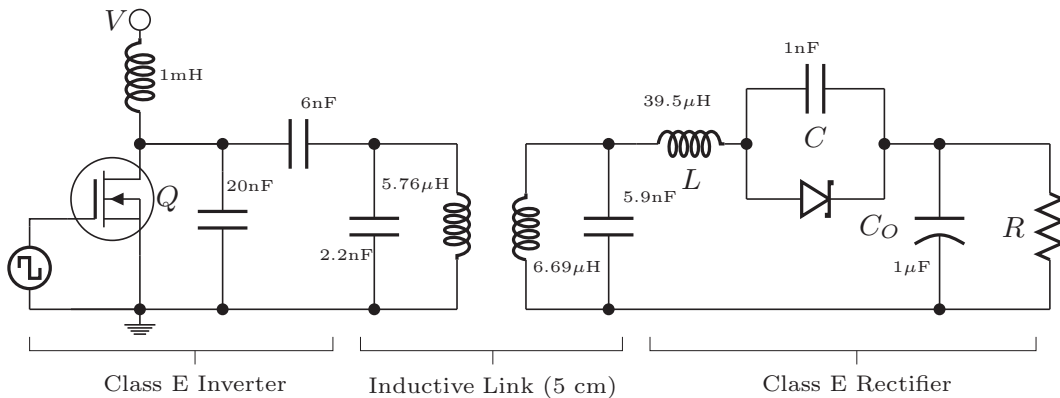Fig. 5. Complete circuit of the IPT system. The circuit consists of a Class E inverter as the transmitting coil current driver, an inductive link with a separation distance of $5\,\mathrm{cm}$ and the designed Class E rectifier.
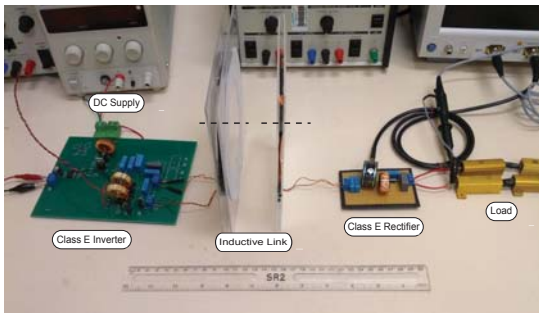

Fig. 6. Photograph of the experimental setup showing the various sections of the IPT system. The DC supply of the Class E inverter is varied to control the inducted voltage at the secondary coil of the inductive link.

IPT systems. A piecewise linear state-space representation has been used to model the rectifier and to derive various parameters. The fidelity of the model is enhanced by the inclusion of the diode's voltage drop, its ON resistance, and the ESR of the resonant inductor in the analysis. A novel investigation into the power quality of the Class E rectifier has been conducted by evaluating parameters such as power factor and THD of its input current which previously were not considered. Such parameters can aid in determining the performance of the Class E rectifier and its effect on the resonant operation of a IPT system.

Experimental results are presented based on a Class E rectifier designed to operate in a resonant IPT system that is capable of delivering up to $10\,\mathrm{W}$. The results are in excellent agreement with the numerical calculations and simulations, thus confirming the analysis and modelling approach. The
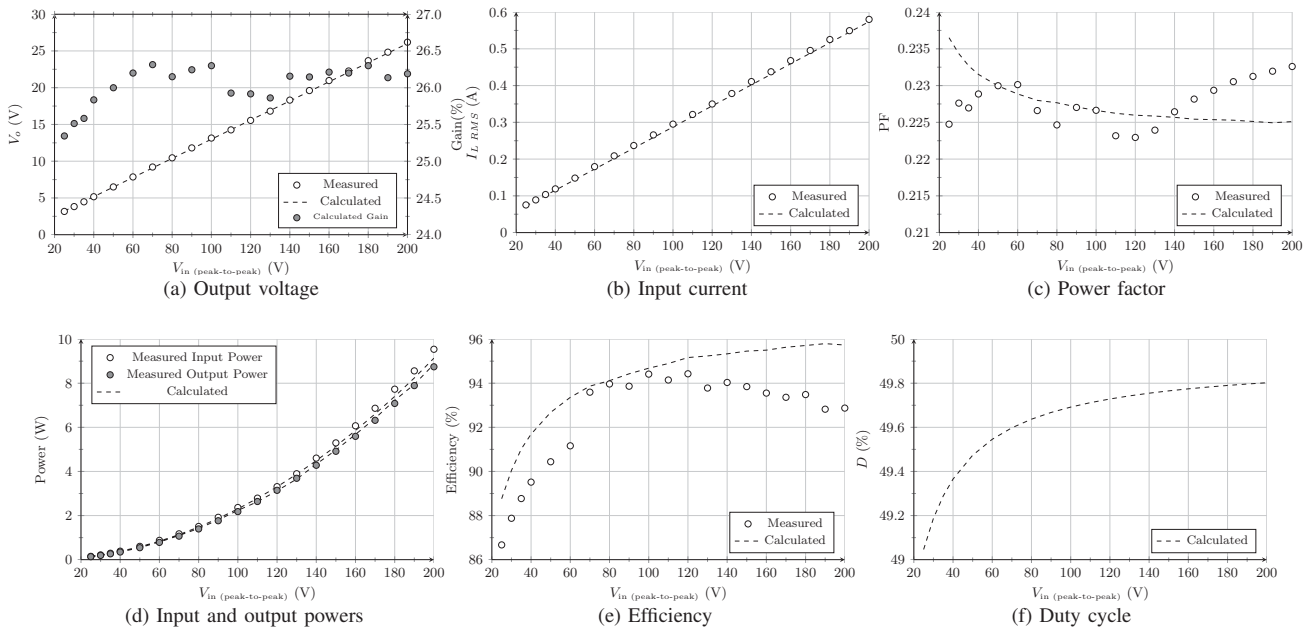
(a) Output voltage

(b) Input current

(c) Power factor

(d) Input and output powers

(e) Efficiency

(f) Duty cycle

Fig. 7. Measured and calculated values of various parameters against input voltage.

(a) Input voltage

(b) Input current

(c) Diode voltage
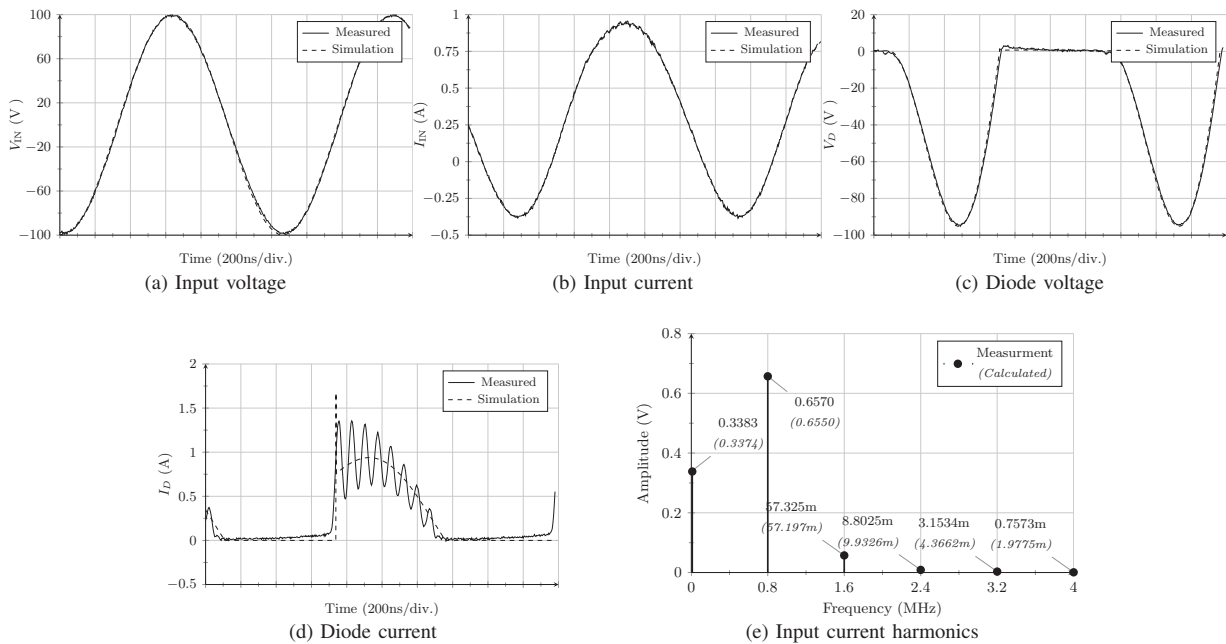
(d) Diode current

(e) Input current harmonics

Fig. 8. Measured and simulated voltages and currents throughout the rectifier for an input voltage of 200 Vpp.

results obtained show that the designed rectifier operates at efficiencies exceeding 90 % over an input voltage ranging from 40 Vpp to 200 Vpp, with a maximum efficiency of 94.43 %.

It is noted that the current work focuses on the performance of the Class E rectifier for resonant inductive links that are applicable to different IPT applications, which is validated by a low power prototype. Thus, future work may include further investigation into higher power applications, such as comprehensive analysis of a complete IPT system for charging electric vehicles. In addition, the diode of the rectifier could

be replaced with a MOSFET to increase the rectifier's input voltage range and output power capability. This can lead to designing a self-powered MOSFET gate driver, timing and control circuitry.

REFERENCES

[1] W. Zhong, C. Zhang, X. Liu, and S. Hui, "A methodology for making a 3-coil wireless power transfer system more energy efficient than a 2-coil counterpart for extended transmission distance," *IEEE Trans. Power Electron*, to be published 2014.

[2] J. Lee, Y.-S. Lim, W.-J. Yang, and S.-O. Lim, "Wireless power transfer system adaptive to change in coil separation," *IEEE Trans. Antennas Propag.*, vol. 62, no. 2, pp. 889–897, Feb. 2014.

[3] C. Park, S. Lee, G. Cho, and C. Rim, "Innovative 5m-off-distance inductive power transfer systems with optimally shaped dipole coils," *IEEE Trans. Power E;ectron.*, to be published 2014.

[4] S. Raju, R. Wu, M. Chan, and C. P. Yue, "Modeling of mutual coupling between planar inductors in wireless power applications," *IEEE Trans. Power Electron.*, vol. 29, no. 1, pp. 481–490, Jan 2014.

[5] W. Zhang, S.-C. Wong, C. K. Tse, and Q. Chen, "Design for efficiency optimization and voltage controllability of series-series compensated inductive power transfer systems," *IEEE Trans. Power Electron.*, vol. 29, no. 1, pp. 191–200, Jan. 2014.

[6] G. A. Covic and J. T. Boys, "Inductive power transfer," *Proc. IEEE*, vol. 101, no. 6, pp. 1276–1289, Jun. 2013.

[7] A. P. Sample, B. H. Waters, S. T. Wisdom, and J. R. Smith, "Enabling seamless wireless power delivery in dynamic environments," *Proc. IEEE*, vol. 101, no. 6, pp. 1343–1358, Apr. 2013.

[8] W. Zhong, C. K. Lee, and S. Y. R. Hui, "General analysis on the use of tesla's resonators in domino forms for wireless power transfer," *IEEE Trans. Ind. Electron.*, vol. 60, no. 1, pp. 261–270, Jan. 2013.

[9] S. Aldhaher, P.-K. Luk, and J. Whidborne, "Tuning Class E inverters applied in inductive links using saturable reactors," *IEEE Trans. Power Electron.*, vol. 29, no. 6, pp. 2969–2978, Jun. 2014.

[10] S. Aldhaher, P. Luk, and A. Bati, "Wireless power transfer using Class E inverter with saturable DC-feed inductor," *IEEE Trans. Ind. Appl.*, to be published 2014.

[11] S. Aldhaher, P. Luk, and J. Whidborne, "Electronic tuning of misaligned coils in wireless power transfer systems," *IEEE Trans. Power Electron.*, to be published 2014.

[12] S. Aldhaher, P. C. K. Luk, and J. F. Whidborne, "Wireless power transfer using Class E inverter with saturable DC-feed inductor," in *Proc. IEEE Energy Convers. Congr. Expo.*, Sep. 2013, pp. 1902–1909.

[13] M. Pinuela, D. C. Yates, S. Lucyszyn, and P. D. Mitcheson, "Maximizing DC-to-load efficiency for inductive power transfer," *IEEE Trans. Power Electron.*, vol. 28, no. 5, pp. 2437–2447, May 2013.

[14] B. L. Cannon, J. F. Hoburg, D. D. Stancil, and S. C. Goldstein, "Magnetic resonant coupling as a potential means for wireless power transfer to multiple small receivers," *IEEE Trans. Power Electron.*, vol. 24, no. 7, pp. 1819–1825, Jul. 2009.

[15] G. A. Kendir, W. Liu, G. Wang, M. Sivaprakasam, R. Bashirullah, M. S. Humayun, and J. D. Weiland, "An optimal design methodology for inductive power link with class-E amplifier," *IEEE Trans. Circuits Syst. I, Reg. Papers*, vol. 52, no. 5, pp. 857–866, May 2005.

[16] J. Huh, S. W. Lee, W. Y. Lee, G. H. Cho, and C. T. Rim, "Narrow-width inductive power transfer system for online electrical vehicles," *IEEE Trans. Power Electron.*, vol. 26, no. 12, pp. 3666–3679, Dec. 2011.

[17] Z. N. Low, R. A. Chinga, R. Tseng, and J. Lin, "Design and test of a high-power high-efficiency loosely coupled planar wireless power transfer system," *IEEE Trans. Ind. Electron.*, vol. 56, no. 5, pp. 1801–1812, May 2009.

[18] M. de Rooij and J. Strydom, "Low power wireless energy converters," White Paper: WP014, EPC, 2013.

[19] S. Birca-Galateanu and A. Ivascu, "Class E low dv/dt and low di/dt rectifiers: energy transfer, comparison, compact relationships," *IEEE Trans. Circuits Syst. I, Fundam. Theory Appl*, vol. 48, no. 9, pp. 1065–1074, Sep. 2001.

[20] M. K. Kazimierczuk and J. J. Jozwik, "Class-E zero-voltage-switching and zero-current-switching rectifiers," *IEEE Trans. Circuits Syst.*, vol. 37, no. 3, pp. 436–444, Mar. 1990.

[21] K. Fukui and H. Koizumi, "Class-E rectifier with controlled shunt capacitor," *IEEE Trans. Power Electron.*, vol. 27, no. 8, pp. 3704–3713, Jan. 2012.

[22] J. Garcia, R. Marante, and M. de las Nieves Ruiz Lavin, "GaN HEMT Class E^2 resonant topologies for UHF DC/DC power conversion," *IEEE Trans. Microw. Theory Techn*, vol. 60, no. 12, pp. 4220–4229, Dec. 2012.

[23] J. Rivas, O. Leitermann, Y. Han, and D. Perreault, "A very high frequency DC-DC converter based on a Class Φ_2 resonant inverter," *IEEE Trans. Power Electron.*, vol. 26, no. 10, pp. 2980–2992, Oct. 2011.

[24] R. Pilawa-Podgurski, A. Sagneri, J. Rivas, D. Anderson, and D. Perreault, "Very-high-frequency resonant boost converters," *IEEE Trans. Power Electron.*, vol. 24, no. 6, pp. 1654–1665, Jun. 2009.

[25] J. J. Jozwik and M. K. Kazimierczuk, "Analysis and design of Class E^2 DC/DC converter," *IEEE Trans. Ind. Electron.*, vol. 37, no. 2, pp. 173–183, Apr. 1990.

[26] M. K. Kazimierczuk and J. J. Jozwik, "Resonant DC/DC converter with class-E inverter and class-E rectifier," *IEEE Trans. Ind. Electron.*, vol. 36, no. 4, pp. 468–478, Nov. 1989.

[27] S. H. Abdelhalem, P. S. Gudem, and L. E. Larson, "An RF-DC converter with wide-dynamic-range input matching for power recovery applications," *IEEE Trans. Circuits Syst. II, Exp. Briefs*, vol. 60, no. 6, pp. 336–340, Apr. 2013.

[28] A. Ivascu, M. K. Kazimierczuk, and S. Birca-Galateanu, "Class E resonant low dv/dt rectifier," *IEEE Trans. Circuits Syst. I, Fundam. Theory Appl*, vol. 39, no. 8, pp. 604–613, Aug. 1992.

Samer Aldhaher received the B.Sc. degree in electrical engineering from the University of Jordan, Amman, Jordan in 2010. He is currently working towards the Ph.D. degree at Cranfield University, Bedford, UK.

His current research interests include the design of high frequency DC/AC inverters, wireless power transfer applications based on resonant inductive links and switched-mode circuits.

Patrick Chi-Kwong Luk (M'92-SM'08) was born in Hong Kong. He received the High Diploma with merits (BSc) in electrical engineering from Hong Kong Polytechnic University, Hong Kong, in 1983, the M.Phil. degree in electrical engineering from Sheffield University, U.K., in 1989, and the Ph.D. degree in electrical engineering from the University of South Wales in 1992.

He started his career in industry in 1983, first as Assistant Engineer at GEC (H.K.) and then Applications Engineer at Polytek Engineering Co. (H.K.). In 1986, he worked as Researcher II in the Industrial Centre, PolyU. Since 1988, he had held academic positions at the University of South Wales, Robert Gordon University, Aberdeen, U.K., and University of Hertfordshire, U.K. He joined Cranfield University, Shrivenham, U.K., in 2002, where he is a Chair Professor in Electrical Engineering and Head of the Electric Power and Drives Group in the School of Engineering. He sits in several IEEE Committees on Electrical Machines and is the Chairman of the IEEE UKRI Young Professionals. He is also an Associate Editor for IEEE Transactions on Power Electronics, IEEE Transactions on Smart Grids, and IET Renewable Power Generation. He has over 140 publications and co-holder of several patents in power electronics, motor drives, and control. His main current research interests include electrical drives, renewable energy systems, and high-frequency power electronics. He is a regular presenter and has been invited keynote speakers at international conferences.

Currently, he is an invited Visiting Professor at Blaise Pascal University in France.

Khalil El Khamlichi Drissi Khalil El Khamlichi Drissi received the Diploma Engineer, M.Sc., and PhD degrees in Electrical Engineering from Ecole Centrale de Lille and the University of Lille, in 1987 and 1990 respectively.

He received the Habilitation in electronics, the highest qualification in France at the Doctoral School 'Sciences Pour l'Ingnieur' of Blaise Pascal University, in 2001. Dr. Khalil El Khanlichi Drissi became Vice President of the Research Vice President of Innovation and Technology Transfer, UBP chancellor board in April 2012. Currently, he is a professor at the Department of Electrical Engineering where he was the dean in the period from 2007 to 2011. He is also a senior researcher at Institute Pascal Laboratory and his research interests include EMC in Power Electronics and Power Systems, in particular; numerical modeling, EMI reduction and converter control.

He has been a member of different scientific societies and President of the SEE Auvergne region since July 2002 (Socit de l'Electricit, de l'Electronique et des Technologies de l'Information et de la Communication) and Senior Member from December 2, 2003. He authored or coauthored more than 100 scientific papers published in peer-review journals and presented at international conferences. Dr. El Khamlichi Drissi is a member of IEEE and EEA and has been a chairperson and member of scientific committees at international conferences. He is a project leader and responsible for several international projects related to EMC (FP7 Marie Curie, Integrafm, Cedre) and a partner within the Brain City Research Institute of South Korea.

He currently has an on-going collaboration with different companies (IFP, EDF, France Telecom and Landis+Gyr).

James F. Whidborne (M'95-SM'10) received the BA in engineering from Cambridge University and MSc and PhD in systems and control from University of Manchester Institute of Science and Technology (UMIST), UK.

From 1991-1994, he was a research associate with the Department of Engineering, University of Leicester. From 1994-2003, he was a lecturer, then senior lecturer with the Department of Mechanical Engineering, Kings College London. He is currently Head of the Dynamics Simulation and Control Group in the Department of Aerospace Engineering at Cranfield University, UK. His research interests are in the theory and application of advanced control, including multi-objective robust control design, fluid flow control, finite precision controller implementation problems, as well as flight control problems such as control and guidance of UAVs, controller reallocation and attitude control of VTOL aircraft.

He is a chartered engineer, a Member of the IET and a Senior Member of the IEEE.

High input voltage high frequency class E rectifiers for resonant inductive links

Aldhaher, Samer